Int J Adv Manuf Technol (2006) 27: 531–536
DOI 10.1007/s00170-004-2210-8

ORIGINAL ARTICLE

Kong-Tian Zuo · Li-Ping Chen · Yun-Qing Zhang · Jingzhou Yang

Manufacturing- and machining-based topology optimization

Received: 28 January 2004 / Accepted: 13 April 2004 / Published online: 11 May 2005

Abstract Topology optimization is used in the initial stage of the product manufacturing process. However, the non-manufacturable or non-machineable results of topology optimization have become an obstacle to process manufacturing. This paper proposes a modified topology optimization method by adding manufacturing and machining constraints to the topology optimization formulation. A hybrid topology optimization algorithm (combining the method of moving asymptotes and wavelets) is applied to solve this optimization problem. With this approach, the design space can be reduced and an engineering-accepted and manufacturable topology result can be guaranteed.

Keywords Machining constraints · Manufacturing constraints · Method of moving asymptotes · Topology optimization

1 Introduction

The popularity of topology optimization methods in structural design has increased rapidly since Bendsoe and Kikuchi's study [1] triggered a renewed interest in the topic.

Currently, topology optimization has rapidly developed and, with the maturation of topology theory and an increased number of tools, it has become a strong method in the design of new products. However, a range of problems, including porosity, a design with checkerboards, mesh dependency, local minimum results, etc. often lead to a non-manufacturable topology that cannot be accepted later in the manufacturing and machining process.

K.-T. Zuo · L.-P. Chen · Y.-Q. Zhang
Center for Computer-Aided Design,
Huazhong University of Science & Technology Wuhan,
Hubei, 430074, P.R. China

J. Yang (✉)
Center for Computer-Aided Design,
The University of Iowa,
Iowa City, IA 52246, USA
E-mail: jyang@engineering.uiowa.edu
Tel.: +1-319-3532249
Fax: +1-319-3840542

Many numerical methods, such as the mesh-independent filter, the slope constraint method and the perimeter constraint [2] can be used to eliminate porosity, checkerboards, and mesh dependency. The local minima are normally resolved by using a different initial point selection. However, even if numerical instability can be fully resolved, the topology result is still not always manufacturable. Because topology design is a concept design process, some manufacturing and machining factors, such as the minimal hole size for machining tools – a characteristic that affects casting and the symmetry property for a part's function – are generally not taken into consideration in the topology optimization process.

Although the non-manufacturable or non-machineable topology result is difficult to resolve, it is important for engineering applications. A new approach to deal with this problem is proposed in this paper, in which manufacturing and machining factors are considered during the optimization process by introducing manufacturing and machining constraints into the topology optimization formulation. With this approach, the non-accepted result in engineering can be avoided, which will be proven using two examples.

2 Topology optimization with manufacturing and machining constraints

2.1 Topology optimization based on SIMP

The solid isotropic material with penalization model (SIMP) method was initially proposed by Mlejnek[3], and Bendsoe and Sigmund [4]. The topology optimization of minimal compliance problem based on SIMP can be written as follows:

$$\begin{aligned} &\text{Minimize}: C = \boldsymbol{U}^T K \boldsymbol{U} = \sum_{e=1}^{N} u^e k^e u^e = \sum_{e=1}^{N} (x^e)^p u^e k_0 u^e \\ &\text{Subject to}: V = f \times V_0 = \sum_{e=1}^{N} x^e v^e \le V^* \\ &\boldsymbol{F} = K\boldsymbol{U},\ 0 < x_{\min} \le x^e \le x_{\max} \end{aligned} \tag{1}$$

where C is the compliance of the structure, $\boldsymbol{F}$ is the force vector, $\boldsymbol{U}$ is the displacement vector, K is the stiffness matrix of the structure, V_0 is the initial volume of the structure, V^* is the maximum volume of the structure, V is the structure's volume after optimization, and f is the ratio of initial volume to volume after optimization. The volume constraint and equilibrium equation of the structure are included. v^e is the element volume after optimization, x^e is the design variable of the element, $x_{\min}$ is the lower bound constraint of element density, introduced to prevent singularity of the equilibrium problem, $x_{\max}$ is the upper bound constraint of element density, u^e is the displacement vector of the node, and N is the total number of discrete elements. Penalty factor p is introduced to increase the cost of intermediate density elements and decrease the number of intermediate density elements, in order to make the density of the elements as close as possible to 0 or 1. By using this SIMP method, the discrete variable optimization problem is changed into a continuous one.

2.2 Manufacturing- and machining-based formulation

The design variable in topology optimization is very large. The objective and constraint always exhibit non-convex behavior, so the design space is also non-convex. The optimization problem in non-convex design space has multiple extrema. A convex approximation method is proven to be efficient for solving the complex large-scale topology optimization problem [5, 6]. This makes the solution an approximation of the initial problem.

In order to deal with a topology result that is non-manufacturable, extra manufacturing and machining constraints are introduced according to the practicality requirement. Such constraints condense the initial design space and the solution in condensed space in order to find an engineering-acceptable result.

A two-dimensional design space without manufacturing and machining constraints is shown in Fig. 1. A convex approximation method is used to approximate the initial design problem. The iteration process of convex approximation is also shown in Fig. 1. Without taking other factors into account that occur later in the manufacturing and machining process, the result $\boldsymbol{X}_1^*$ can at times be useless from an engineering standpoint. Figure 2 is a condensed design space with manufacturing and machining constraints, in which a convex approximation method and its solution iteration are included. The result $\boldsymbol{X}_2^*$ has taken manufacturing and machining factors into consideration and is useful from an engineering perspective. The result $\boldsymbol{X}_2^*$ is therefore different from $\boldsymbol{X}_1^*$.

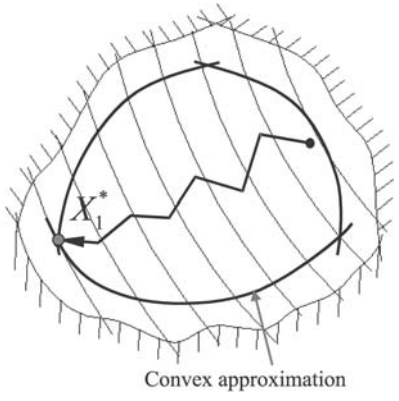

Fig. 1. Design domain without manufacturing constraints

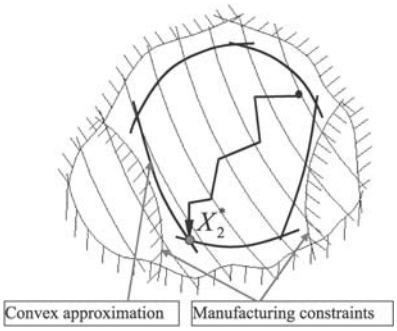

Fig. 2. Design domain with manufacturing constraints

The formulation of topology optimization with manufacturing and machining constraints can be written as follows:

$$\begin{aligned}
&\text{Minimize}: C = \boldsymbol{U}^T K \boldsymbol{U} = \sum_{e=1}^{N} u^e k^e u^e = \sum_{e=1}^{N} (x^e)^p u^e k_0 u^e \\
&\text{Subject to}: V = f \times V_0 = \sum_{e=1}^{N} x^e v^e \le V^* \\
&\qquad \boldsymbol{F} = K\boldsymbol{U},\ 0 < x_{\min} \le x^e \le x_{\max} \\
&\qquad g(x^e) - g_0 \le 0,\ h(x^e) = 0
\end{aligned} \tag{2}$$

where $g(x^e) - g_0 \le 0$ and $h(x^e) = 0$ are manufacturing and machining constraints.

Forms of manufacturing and machining constraints are different for different applications. Some constraints, such as minimal size constraint, symmetrical constraint, conforming constraint, etc., can be introduced into the optimization according to the various requirements of application problems.

2.3 Numerical solver

Once manufacturing and machining constraints are added to the single-constraint design problem in optimization, it becomes a multiple-constraint problem. It can now be solved with an advanced mathematical programming method, such as the method of moving asymptotes (MMA) [7, 8]. However, the MMA algorithm used for topology optimization is not globally convergent. As a result, some global numerical instabilities and convergence problems may appear that may necessitate an effective global filter. Multi-resolution is an important characteristic of a wavelet, which can be used as a global filter for the design variable and its sensitivity. We use a hybrid approach of wavelet and MMA, in which some information in the design, such as numerical instability, can be removed using the filter characteristic of the wavelet.

The design variable in two-dimensional topology optimization can be represented with $f(x, y)$, which can be approximated

using a multi-resolution approximation in $L^2(R \times R)$ with a sequence of subspaces $\{V_j(x, y)\}_{j \in Z}$ (where R is the set of real numbers and Z is the set of integers). The two-dimensional base function for multi-resolution can be defined as:

$$\phi_{j,m}(x)\phi_{j,n}(y) = 2^{j/2}\phi(2^j x - m)2^{j/2}\phi(2^j y - n) \tag{3}$$

where $\phi(2^j x - m)$ and $\phi(2^j y - n)$ are one-dimensional base functions, $j, m, n \in Z$, and function $f(x, y)$ can be approximated as:

$$f^j(x, y) = \sum_{m,n} c^j_{m,n}\phi_{j,m}(x)\phi_{j,n}(y) \tag{4}$$

where $f^j(x, y) \in V_j(x, y)$, and $c^j_{m,n}$ denotes component coefficients on nodes.

The following decomposing relations exist for the multi-resolution of two-dimensional wavelets:

$$V_{j+1}(x, y) = V_j(x, y) \oplus W_j(x, y) \tag{5a}$$
$$W_j(x, y) = V_{j+1}(x, y)/V_j(x, y) \tag{5b}$$

where $W_j(x, y)$ is the orthogonal complement of $V_j(x, y)$ in $V_{j+1}(x, y)$.

The approximating function $f^{j+1}(x, y) \in V_{j+1}(x, y)$ can be decomposed into four parts in $V_j(x, y)$-space and $W_j(x, y)$-space, respectively as:

$$\begin{aligned} V_{j+1}(x, y) =& V_{j+1}(x) \otimes V_{j+1}(y) \\ =& [V_j(x) \oplus W_j(x)] \otimes [V_j(y) \oplus W_j(y)] \\ =& [V_j(x) \otimes V_j(y)] \oplus [V_j(x) \otimes W_j(y) \oplus W_j(x) \\ & \otimes V_j(y) \oplus W_j(x) \otimes W_j(y)] \end{aligned} \tag{6}$$

where $\oplus$ represents the direct sum, and $\otimes$ represents the tensor product.

When $\phi(x, y)$ is an orthogonal scaling function, the base function in spaces $V_j(x, y)$ and $W_j(x, y)$ can be written as:

$$\begin{aligned} V_j(x, y) &= V_j(x) \otimes V_j(y) \\ &= \text{span}\left\{\phi_{j,m}(x)\phi_{j,n}(y),\ m, n \in Z\right\} \end{aligned} \tag{7a}$$
$$\begin{aligned} W^1_j(x, y) &= V_j(x) \otimes W_j(y) \\ &= \text{span}\left\{\phi_{j,m}(x)\psi_{j,n}(y),\ m, n \in Z\right\} \end{aligned} \tag{7b}$$
$$\begin{aligned} W^2_j(x, y) &= W_j(x) \otimes V_j(y) \\ &= \text{span}\left\{\psi_{j,m}(x)\phi_{j,n}(y),\ m, n \in Z\right\} \end{aligned} \tag{7c}$$
$$\begin{aligned} W^3_j(x, y) &= W_j(x) \otimes W_j(y) \\ &= \text{span}\left\{\psi_{j,m}(x)\psi_{j,n}(y),\ m, n \in Z\right\} \end{aligned} \tag{7d}$$

where $\phi_{j,m}$ and $\phi_{j,n}$ are the orthogonal bases in $V_j(x)$ by scaling and translating from the scaling function ϕ, and $\psi_{j,m}(x)$ and $\psi_{j,n}(x)$ are the orthogonal bases in $W_j(x)$ constructed from the wavelet function ψ.

In this paper, the Daubechies orthogonal wavelet is used to approximate the function of density distribution in topology optimization.

From Eqs. 4 to 7d, one can obtain

$$\begin{aligned} f^{j+1}(x, y) =& \sum_{m,n} c^j_{m,n}\phi_{j,m}(x)\phi_{j,n}(y) \\ &+ \sum_{m,n} \alpha^j_{m,n}\phi_{j,m}(x)\psi_{j,n}(y) \\ &+ \sum_{m,n} \beta^j_{m,n}\psi_{j,m}(x)\phi_{j,n}(y) \\ &+ \sum_{m,n} \gamma^j_{m,n}\psi_{j,m}(x)\psi_{j,n}(y) \end{aligned} \tag{8}$$

with an orthogonal scaling function and wavelet, the following decomposing coefficients are obtained:

$$c^j_{m,n} = \sum_{k,l} h(k - 2m)h(l - 2n)c^{j+1}_{k,l},$$
$$\alpha^j_{m,n} = \sum_{k,l} h(k - 2m)g(l - 2n)c^{j+1}_{k,l},$$
$$\beta^j_{m,n} = \sum_{k,l} g(k - 2m)h(l - 2n)c^{j+1}_{k,l},$$
$$\gamma^j_{m,n} = \sum_{k,l} g(k - 2m)g(l - 2n)c^{j+1}_{k,l}$$

The corresponding composing algorithm can be written as:

$$\begin{aligned} c^{j+1}_{m,n} =& \sum_{k,l} c^j_{k,l}h(m - 2k)h(n - 2l) \\ &+ \sum_{k,l} \alpha^j_{k,l}h(m - 2k)g(n - 2l) \\ &+ \sum_{k,l} \beta^j_{k,l}g(m - 2k)h(n - 2l) \\ &+ \sum_{k,l} \gamma^j_{k,l}g(m - 2k)g(n - 2l) \end{aligned} \tag{9}$$

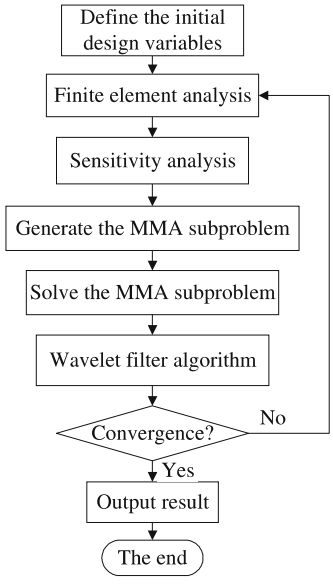

Fig. 3. Flowchart of hybrid algorithm

Therefore, $\{c_{m,n}^{j+1}\}$ in level $j+1$ can be obtained from $\{c_{k,l}^{j}\}$, $\{\alpha_{k,l}^{j}\}$, $\{\beta_{k,l}^{j}\}$, and $\{\gamma_{k,l}^{j}\}$ in level j. In the same way, $\{c_{m,n}^{j+2}\}$ in level $j+2$ can be obtained from $\{c_{m,n}^{j+1}\}$, $\{\alpha_{k,l}^{j+1}\}$, $\{\beta_{k,l}^{j+1}\}$, and $\{\gamma_{k,l}^{j+1}\}$. This algorithm is called multi-resolution analysis in the wavelet. This algorithm is applied as follows: the design function can first be decomposed, and then recomposed, by choosing a threshold and modifying the corresponding coefficients. Numerical instabilities and singular optima involved in the calculation can be removed with decomposing and composing algorithms in the wavelet. In the same way that a noise-eraser works in image processing, a wavelet decomposing and composing algorithm can be viewed as a global filter that can filter or modify the numerical instabilities in function values and their derivatives. It is for this reason that the wavelet algorithm can improve the convergence of the MMA approach. The wavelet decomposing and composing algorithm is added at the end of the MMA approach shown in Fig. 3.

3 Examples

In this section, we will use two illustrative examples to demonstrate the proposed approach for manufacturing- and machining-based topology optimization and the hybrid numerical algorithm to solve this optimization problem. The first is an example of manufacturing constraints, while the second applies machining constraints.

Example 1: Optimization with a machining constraint

A minimal feature size is needed in machining, since a feature whose size is smaller than the minimal value is difficult to cast or machine with tools. Some small features, such as small holes, are often included in topology optimization results, making the result difficult to machine during the subsequent processing. Therefore, it is necessary to introduce a minimal machining hole size constraint in topology optimization to control the formation of small holes.

A finite element model of a 3D cantilever beam is shown in Fig. 4. The beam is clamped at one end and is subject to a force F at the center of the other end. The objective is to minimize the compliance subject to a volume fraction constraint of 0.5 and a minimal machining hole size constraint. The beam is meshed into 160 pentahedron elements and 1040 hexahedron elements.

The result without a machining constraint is shown in Fig. 5, in which a small hole exists. This small hole is not only useless, but it also makes the later casting and machining process difficult to perform. The hole can be eliminated with a minimal hole constraint added into the optimization formulation. The result with the machining constraint is shown in Fig. 6. The hole in the middle of the beam disappears, and the result is beneficial for later machining.

In this example, a minimal hole size constraint for machining can be written as follows:

$$G = \frac{\sum_{k=1}^{M} s_k \times x_k^e}{l^p} \geq G^* \tag{10}$$

where G is an equivalent hole size of discrete boundary elements with respect to projection plane P, s_k is the exterior surface area of boundary element k, M is the number of boundary elements, l^p is the average depth of the boundary hole with respect to projection plane P, and G^* is the lower bound of the minimal hole size, determined by extensive practical requirements. Projection plane P is defined as the yz-plane that is controlled by the minimal machining size. As mentioned above, a lower bound value of the minimal machining size is introduced to control the minimal feature size in topology optimization results.

Example 2: Optimization with a manufacturing constraint

Because some manufacturing parts are symmetrical or conform in structure or function, a symmetrical or conforming topology optimization result should benefit their further design and manufacture. Such results are possible by adding a symmetrical or conforming constraint into the optimization formulation.

The finite element model of a hook in a space mechanism and its design domain are shown in Fig. 7. The hook is fixed at the foot, subject to a surface pressure F on the joggled surface of the head. Two design domains and two non-design domains are included in this model. The joggled surface of the head, where pressure F is loaded, and the foot, which is connected to another

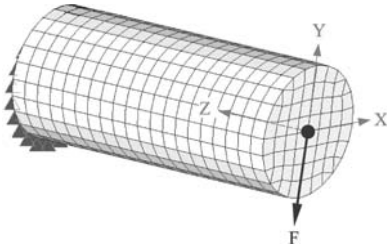

Fig. 4. Finite element model showing the machining constraint and design domain

Fig. 5. Result without a machining constraint

Fig. 6. Result with a machining constraint

part, compose the non-design domains, whose shape and size are unchangeable. The two areas exempt from non-design domains are design domains. The density of the elements in non-design domains are set as constant and do not change with the number of iterations, while the density of elements in design domains are changeable.

The object is to minimize the compliance subject to a volume fraction constraint of 0.5, a conforming constraint in the z-direction of the head, and a symmetrical constraint in the z-direction of the tail. Conforming constraints on the head mean that the density of different elements in the same z-direction of a fixed (i, j) position are equal. Symmetrical constraints on the tail mean that the density of whole elements is symmetrical with respect to the xy-plane. The hook is meshed into 60 pentahedron elements and 11 150 hexahedron elements.

The result without manufacturing constraints is shown in Fig. 8. The topology distribution is irregular and complex on the head as well as on the tail. This result is difficult to use for further design and manufacturing purposes. The result with a conforming constraint on the head and a symmetrical constraint on the tail is shown in Fig. 9. In this figure, the density of elements at the head is equal in the z-direction to the tail, and is symmetrical with respect to the xy-plane.

In this example, the conforming constraint can be expressed as:

$$\sum_{k=1}^{K1-1} \left| (x_{ij}^e)_{k+1} - (x_{ij}^e)_k \right|_p \le \delta,\ i = 1, \ldots, n_x,\ j = 1, \ldots, n_y \tag{11}$$

where $(x_{ij}^e)_k$ is the density of the kth element at the (i, j) position of perpendicular projection plane P, which is written as the xy-plane here, $K1$ is the number of elements at the (i, j) position, n_x, n_y are the number of elements in the x and y direction on the projection plane, respectively, and δ is a small positive number.

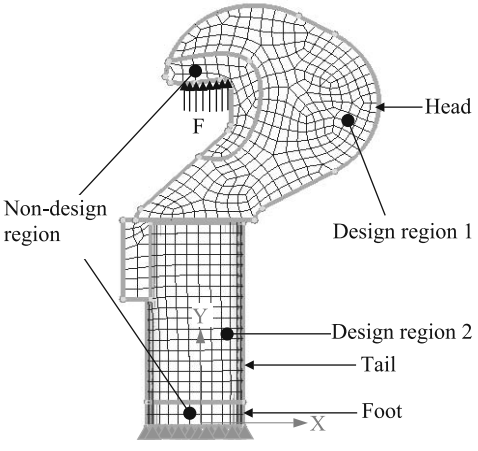

Fig. 7. Finite element model showing the manufacturing constraint and design domain

In this example, the symmetrical constraint can be expressed as:

$$\sum_{k=1}^{K2} \left| (x_{ij}^e)_k - (x_{ij}^e)_{-k} \right|_M \le \delta,\ i = 1, \ldots, n_x,\ j = 1, \ldots, n_y \tag{12}$$

where $(x_{ij}^e)_{-k}$ is the element density that is opposite to $(x_{ij}^e)_k$ with respect to symmetrical plane M, which is the xy-plane in this example, and $K2$ is the sequence number of elements at the (i, j) position.

The result of topology optimization should be smoothed and reconstructed before further detailed design, manufacturing, and machining takes place. Figure 10 is a finite element model after reconstruction on the basis of the topology results.

With extra constraints introduced into the optimization formulation, calculation costs rapidly increase. Moreover, the lower bound G^* in the minimal machining size constraint is not easy to define, and requires experience and a detailed understanding of the requirements.

Fig. 8. Result without manufacturing constraints

Fig. 9. Result with manufacturing constraints

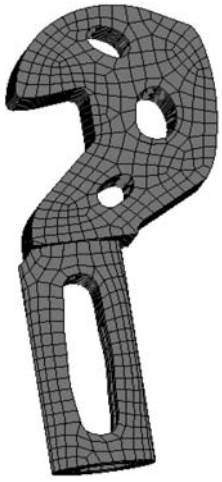

Fig. 10. Reconstructed finite element model based on the topology results

4 Conclusion

This paper has illustrated that the use of manufacturing and machining constraints in topology optimization can solve non-manufacturing and non-machining problems in engineering applications. In addition, it has shown that the hybrid algorithm can overcome the disadvantage of a pure MMA method and effectively improve convergence. The topology optimization results with manufacturing and machining constraints can guarantee engineering requirements and benefit the subsequent design, manufacturing, and machining process.

References

1. Bendsoe M, Kikuchi N (1988) Generating optimal topologies in structural design using a homogenization method. Comput Methods Appl Mech Eng 71:197–224
2. Sigmund O, Petersson J (1998) Numerical instabilities in topology optimization: a survey on procedures dealing with checkerboards, mesh-dependencies and local minima. Struct Optim 16:68–75
3. Mlejnek HP, Schirrmacher R (1993) An engineering approach to optimal material distribution and shape finding. Comput Methods Appl Mech Eng 106:1–26
4. Bendsoe MP, Sigmund O (1999) Material interpolations in topology optimization. Arch Appl Mech 69:635–654
5. Fleury C (1993) Sequential convex programming for structural optimization problems. In: Rozvany GIN (ed.) Optimization of large structural systems. Kluwer, Dordrecht, pp 567–578
6. Bruyneel M, Fleury C (2002) Composite structures optimization using sequential convex programming. Adv Eng Softw 33:697–711
7. Svanberg K (1987) The method of moving asymptotes – a new method for structural optimization. Int J Numer Meth Eng 24:359–373
8. Svanberg K (1999) The MMA for modeling and solving optimization problems. In: Proceedings of the Third World Congress on Structural and Multidisciplinary Optimization, Buffalo, New York